

Integrated Model, Batch and Domain Parallelism in Training Neural Networks

Amir Gholami¹, Ariful Azad², Peter Jin¹, Kurt Keutzer¹, and Aydın Buluç^{1,2}

¹ EECS Department, UC Berkeley, ² CRD, Lawrence Berkeley National Laboratory

Abstract

We propose a new integrated method of exploiting model, batch and domain parallelism for the training of deep neural networks (DNNs) on large distributed-memory computers using minibatch stochastic gradient descent (SGD). Our goal is to find an efficient parallelization strategy for a fixed batch size using P processes. Our method is inspired by the communication-avoiding algorithms in numerical linear algebra. We see P processes as logically divided into a $P_r \times P_c$ grid where the P_r dimension is implicitly responsible for model/domain parallelism and the P_c dimension is implicitly responsible for batch parallelism. In practice, the integrated matrix-based parallel algorithm encapsulates these types of parallelism automatically. We analyze the communication complexity and analytically demonstrate that the lowest communication costs are often achieved neither with pure model nor with pure data parallelism. We also show the positive effect of our approach in the computational performance of SGD based DNN training where the reduced number of processes responsible for data parallelism result in “fatter” matrices that enable higher-throughput matrix multiplication.

1 Introduction and Background

Neural Networks (NNs) have proved to be very effective in diverse applications ranging from semantic segmentation [14, 23] and detection [17, 22] to medical image segmentation [9, 15]. In most cases the hardware limits have been reached for most of the kernels, and the next milestone is in distributed computing. Given N empirical samples, the DNN training procedure seeks to find the model parameters, w , such that the forward pass on sample inputs would produce outputs that are *similar* to ground truth outputs and that it generalizes well for unseen test samples. The weights are initialized randomly and SGD algorithm updates them iteratively as: $w^{n+1} = w^n - \eta \nabla f_i$, where i is an index chosen randomly (with replacement) from $[1, N]$, η is the learning rate, and f is the loss function. In practice, one can use a mini-batch SGD by drawing a set of indices $i \in B$ at each iteration, chosen randomly from $[1, N]$ and update the parameters as follows:

$$w^{n+1} = w^n - \eta \frac{1}{|B|} \sum_{i \in B} \nabla f_i, \quad (1)$$

where $|B|$ is the mini batch size. This whole SGD-based training requires a “forward pass” where the network’s output and the corresponding loss functional is computed given the current model parameters, and a “backward pass” (commonly referred to as *backpropagation* or simply *backprop*) where the gradient of the loss is computed with respect to the model parameters, w .

The forward phase of DNN training is a sequential combination of affine transformation $Y_i = W_i X_i$, and $X_{i+1} = f(Y_i)$ followed by nonlinear transforms, where $X_i \in \mathbb{R}^{d_{i-1} \times B}$, $y_i \in \mathbb{R}^{d_i \times B}$, and $W_i \in \mathbb{R}^{d_i \times d_{i-1}}$. Here, d_i is the activation size of the i th DNN layer. This is followed by backpropagation that can also be written in matrix form as $\Delta_X = W_i^T \Delta_Y$. Here, Δ_X and Δ_Y are the gradients of the loss function, with respect to input and output activations, respectively. Finally, the gradient of the loss function with respect to model weights is calculated using $\Delta_W = \Delta_Y X^T$. Consequently, DNN

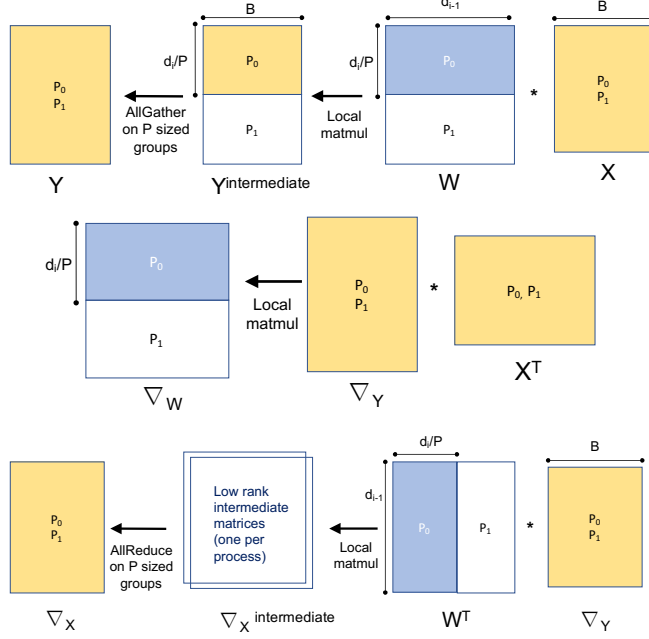


Figure 1: Illustration of matrix multiplications for the pure model parallel training using $P = 2$ (top: forward pass, middle/bottom: weight gradient computation).

training requires 3 *matrix multiplications*, including gradient computations¹. The derivations of the forward pass and the backpropagation are shown in detail in Sections 6.1 and 6.2, respectively.

A single pass over the whole data (also called an *epoch*) requires $N/|B|$ iterations. It takes many iterations until the training error is sufficiently small. Consequently, DNN training is computationally expensive. To accelerate training, one can change the training algorithm with an aim to reduce the number of epochs, or make each epoch run faster through distributed training. We are focusing on the latter.

Two well-known techniques for distributed SGD based DNN training are *model parallelism* and *data parallelism*. In simplest terms, model parallelism is the partitioning of the weights of the neural network to processes. Data parallelism corresponds to partitioning of the data to processes. The existing literature merely considers data parallelism to be the assignment of groups of whole data points, such as images, to individual processes. However, one can instead assign fractions of data points to processes as well. For example, training a convolutional neural network (CNN) on two processes with domain parallelism can assign all the top halves of the images to the first processor and all the bottom halves of the images to the second processor. Consequently, there are two subtypes of data parallelism: *batch parallelism*, which is the commonly studied option in literature, is the assignment of groups of data points in whole to processes and *domain parallelism* is the subdivision of individual data points to processes.

This paper presents a new method for integrated model, batch, and domain parallelism. There are existing approaches that exploit both model and batch parallelism but they often only provide ad-hoc solutions to hard engineering constraints such as the model no longer fitting into a single GPU or the minibatch sizes hitting a convergence limit. Our method, by contrast, is amenable to precise communication analysis and covers the whole spectrum between pure data parallelism (which includes batch parallelism as a special case) and pure model parallelism. It often finds favorable performance regimes that are better than pure batch parallelism and pure model parallelism, even in the absence of hard engineering constraints.

¹Note that our approach does not require each individual convolution to be computed using matrix multiplication, but we view it as this way for simplicity and connection to high performance computing literature.

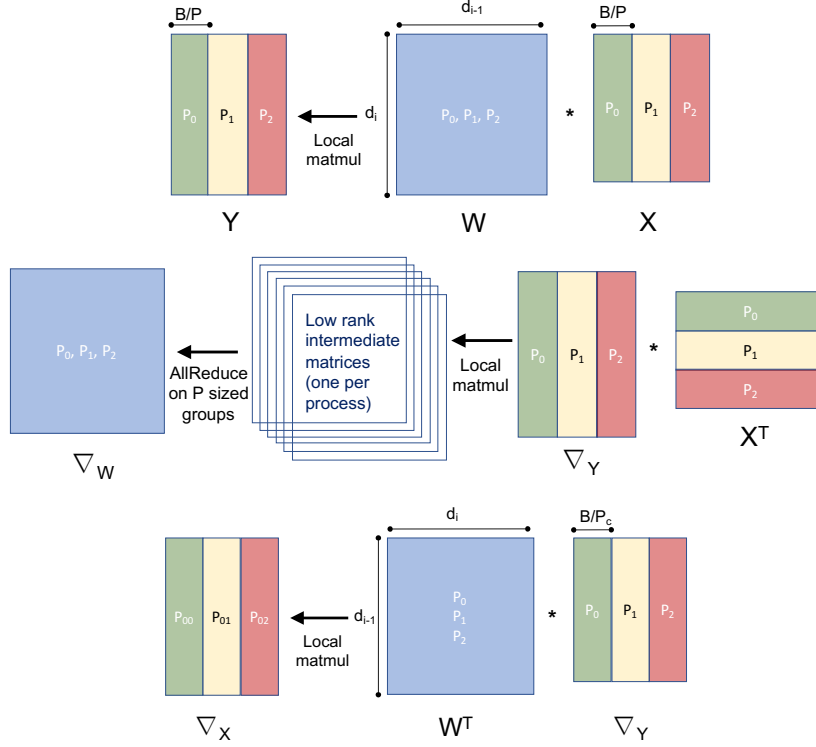


Figure 2: Illustration of matrix multiplications for the pure batch parallel training using $P = 3$ (top: forward pass, middle/bottom: weight gradient computation).

Limitations

We find it useful and necessary to describe the limitations in our analysis. For the communication complexity we assume that all the compute nodes are connected and thus do not consider the topology of the interconnect, and we also do not consider network conflicts in our model [3]. However, the effects of this can be approximated by adjusting the latency and bandwidth terms accordingly, as a detailed analysis will become network specific. Furthermore, the present analysis is only performed on AlexNet, although a future version of this report will include other networks such as ResNet family as well [10]. Moreover, we experimentally measure the computation time. A more detailed analysis of the computation time would require a hardware specific execution model which is outside the scope of this work. Finally, we present simulation results based on the complexity analysis. The implementation of the algorithm is an on-going effort and we will report measured runtimes in a future version of this report.

2 Parallelism in DNN Training using SGD

The SGD iterations have a sequential dependency. One possibility to break this barrier for parallel training is the family of asynchronous SGD methods [18, 11, 16, 4, 7, 25]. Here, this dependency is broken and each process is allowed to use *stale* parameters and update either its weights or that of a parameter server. Here, we focus only on synchronous SGD which obeys the sequential consistency of the original algorithm. However, the framework that we present can be used to accelerate asynchronous methods as well.

In terms of terminology, we use the word “process” to refer to the program running on a compute node. It is often the case that a compute node has many processing elements (or cores); thus one can map multiple processes, each with its own local private memory, to a compute node. The exact nature of process to compute node mapping is immaterial to our analysis.

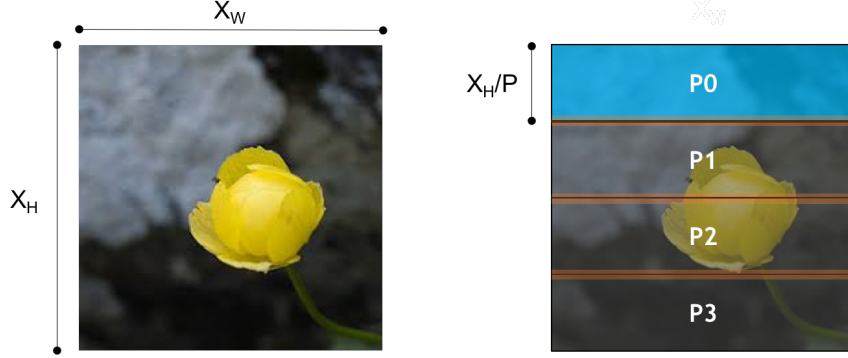


Figure 3: Illustration of domain parallel approach for $P = 4$. For NCHW format, it is best to distributed along the height to avoid inconiguous memory accesses. The shaded orange part shows the halo exchange boundary.

2.1 Communication Cost Analysis of Pure Batch, Pure Model, and Pure Domain-Parallel Approaches

Two possibilities for parallel computations in synchronous SGD is model and data parallel. In the model parallel case, the computation of the loss functional in the forward pass can be computed by distributing the model parameters W as shown in Fig. 1.

Consider a convolutional layer without loss of generality: each process performs a subset of the convolutions on the input activations and computes a subset of the output activations. For instance, assume one of the layers consists of $C^o k_h \times k_w \times C^{in}$ convolutions, where k_h, k_w is the convolution size and C^{in}, C^{out} is the size of input/output channels. In the model parallel case, the kernels are distributed so that each process gets C^o/P filters and computes C^o/P channels of the output activation. As computations of the other layers would require access to all of the previous activations, one needs to perform an all-gather operation *per layer*. Backpropagation also requires an all-reduce communication during Δ_X calculation, as will be discussed later. This yields the following communication complexity for the model parallel case:

$$T_{comm}(model) = 3 \sum_{i=0}^L \left(\alpha \lceil \log(P) \rceil + |B| \frac{P-1}{P} \beta d_i \right), \quad (2)$$

where P is the number of processes, L is the number of DNN layers, α is the network latency, and β is the inverse bandwidth. This analysis assumes the use of Bruck’s algorithm for all-gather and ring algorithm for all-reduce [20]. We note that the complexity depends on the mini-batch size. The model parallel approach was partially used in AlexNet [13], where the model was split into two GPUs. The original GoogLeNet work also exploited a certain amount of model parallelism [19]. Distributed DNN training engines that rely solely on model parallelism also exist [5], especially for low-latency high-bandwidth systems.

The other possibility for distributing the SGD computation is data parallelism. This can be performed either by distributing the data over the batch size, or partition each individual image. We refer to the latter as *domain parallelism*, which will be discussed further below.

For the batch parallel case, the reduction for the gradient computation over the mini-batch sum (1) can be computed independently by each process. This approach is known as *batch parallel* method, where each process computes a partial sum, followed by an all-reduce to compute the mini-batch gradient. This communication cost is due to the reduction that is needed to form $\Delta_W = \Delta_Y X^T$ product. The communication complexity for the batch parallel approach using ring algorithm for all-reduce [20] is:

$$T_{comm}(batch) = 2 \sum_{i=0}^L \left(\alpha \lceil \log(P) \rceil + \frac{P-1}{P} \beta |W_i| \right), \quad (3)$$

where $|W_i|$ is the total number of model parameters in the i th layer. Here, the factor of 2 is merely due to the all-reduce algorithm. Note that for $P \gg 1$ the bandwidth costs are independent of P and does not depend on the batch size. Most of the current work on distributed training uses batch parallel to scale training [8, 24]. The DistBelief paper [7] provides easy-to-understand descriptions of model and batch parallelism.

A third possibility for parallelization, is to decompose the input activation map as shown in Fig. 3. Here each process contains all of the model parameters (as in the pure batch parallel case), but performs the convolutions only on a subset of the input image, and writes a subset of the output activations. For convolutions with filter size larger than one, we have to perform a halo exchange to communicate the boundary points. This can be performed as a non-blocking, pair-wise exchange while the convolution is being applied to the rest of the image. This means that the convolutions that do not require this boundary data could be computed while the communication is being performed. The cost of the communication in this case will be:

$$\begin{aligned} T_{comm}(domain) = & \sum_{i=0}^L (\alpha + \beta |B| X_W^i X_C^i \lfloor k_h^i/2 \rfloor) \\ & + \sum_{i=0}^L (\alpha + \beta |B| Y_W^i Y_C^i \lfloor k_w^i/2 \rfloor) \\ & + 2 \sum_{i=0}^L \left(\alpha \lceil \log(P) \rceil + \frac{P-1}{P} \beta |W_i| \right), \end{aligned} \quad (4)$$

where $X_W^i, X_H^i, Y_W^i, Y_H^i$ are the input/output activation's width and height in the i th layer, and k_h^i, k_w^i is the corresponding convolution size of that layer. Note that for a 1×1 convolution no communication is needed. For layers with large input activation size and large number of convolution filters, this approach can reduce the computation time with good strong scaling efficiency. However, it is not effective for small image sizes and not applicable to fully connected layers.

Model parallelism, as published in literature, corresponds to performing a 1D distribution of the matrix W_i , replicating X_i and gathering Y_i multivectors after multiplication. The k th processor can perform its local matrix multiplication of the form $W_i(k, :) X_i$ without any communication, but in order to fully assemble Y_i , each processor needs to gather other components from other processes. Even if input/output multivectors were also distributed, the communication bounds stay the same, because while this communication time would not be necessary for the output Y_i , it would be needed for gathering X_i before the local multiplication.

By contrast, in data parallelism, every process starts with the same parameters, which get updated by the same gradient. In fact, the forward pass of batch parallel needs no communication. The communication in this case happens during backpropagation, where a collective all-reduce operation is needed to compute the total sum of the partial gradients. The parallel matrix multiplications in the batch parallel case are illustrated in Figure 2.

2.2 Integrated Model and Batch Parallelism

We first discuss the integrated model and batch parallelism and then discuss the full integration with domain parallelism which yields better communication cost. Batch parallelism has a favorable communication complexity, but there is an inherent limit on increasing the batch size. Furthermore, small batch size training is not efficient in terms of hardware utilization and ultimately training time. This is due to the fact that small matrix-matrix operations (aka level-3 BLAS operations) cannot use all the hardware resources, in terms of cores or vectorized units. This is empirically shown in Fig. 4, where we report one epoch training time of AlexNet for different batch sizes measured on a single Intel Knights Landing (KNL) processor. The fastest training time is achieved with a batch size of 256. With the batch parallel approach one has no choice but to reduce per process batch size for scaling before hitting the limit of 1 batch per process.

Our *integrated batch and model parallel approach* allows us to increase the number of efficiently-utilized processors, independently of the batch size. Here, we consider replicating a subset of W_i as opposed to all of it, a concept that has been explored under the name of 1.5D algorithms for

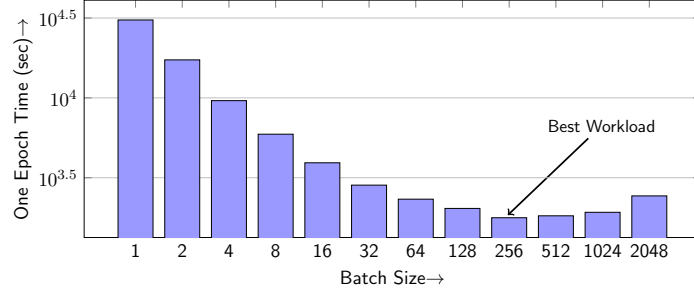


Figure 4: One epoch training time of AlexNet computed on a single KNL. Increasing batch size up to 256, reduces the time due to better use of hardware resources and fewer SGD updates.

matrix multiplication [12]. We think of our process grid logically partitioned as $P = P_r \times P_c$. Each process holds $(1/P_r)$ th piece of W_i , effectively replicating W_i matrix P_c times (as opposed to P times in batch parallelism). Conversely, data matrices are replicated P_r times and each process holds $(1/P_c)$ th piece of X_i and Y_i . Communication cost of this 1.5D algorithm, which is illustrated in Figure 5, is:

$$T_{comm} = 3 \sum_{i=0}^L \left(\alpha \lceil \log(P_r) \rceil + |B| \frac{P_r - 1}{P_r} \beta \frac{d_i}{P_c} \right) + 2 \sum_{i=0}^L \left(\alpha \lceil \log(P_c) \rceil + \frac{P_c - 1}{P_c} \beta \frac{|W_i|}{P_r} \right). \quad (5)$$

This provides a theoretically sound integration of batch and model parallelism. It can be especially valuable when the batch parallelism hits limits due to convergence issues with very large batch sizes. Furthermore, this algorithm automatically selects the best configuration to distribute the model and batch parallel work given a fixed batch size on P processes. The closest approach to ours is the hybrid model/batch parallel approach described by Das et al. [6], but that paper does not describe the details of the partitioning of the data and the model to the processes. In addition, the authors claim that using any other dimension to extract parallelism would always be sub-optimal, which we show not be true in general by using domain parallelism.

For the curious reader familiar with the theory of parallel matrix multiplication, we would like to clarify why we consider our approach a 1.5D algorithm, as opposed to a 2D algorithm such as Cannon’s algorithm [2] or SUMMA [21]. 2D matrix multiplication algorithms are optimal in terms of their memory usage; that is, each processor only holds $(1/p)$ th of the total memory needed to store all three matrices (2 inputs and 1 output). In other words, there is no replication. The class of .5D algorithms (of which 1.5D algorithm is a member), by contrast, are not optimal in terms of memory consumption. At least one matrix is replicated multiple times, which often results in an asymptotic reduction in communication costs [1]. This is indeed the case for the algorithm described in Figure 5.

2.3 Integrated Model, batch and Domain Parallelism

The domain parallel approach has a favorable communication complexity for early layers of a neural network where the input activation size is large. For these layers it is favorable to use domain parallelism instead of model parallel, as it leads to a smaller non-blocking communication. Note that in model parallel one has to perform a blocking all-gather operation which is detrimental for performance. The communication complexity for integrating all the three methods would then become:

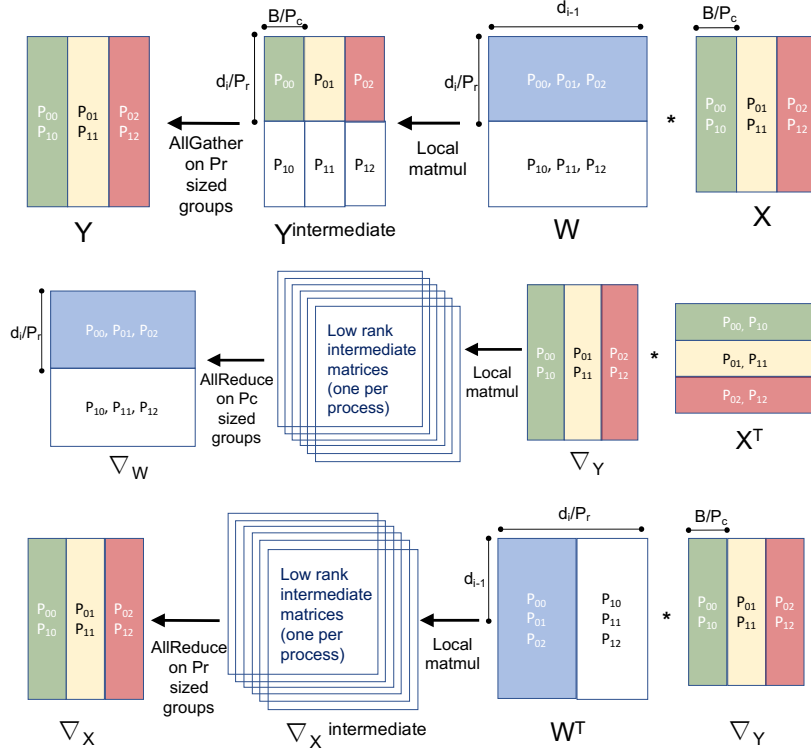


Figure 5: 1.5D matrix multiply illustration for integrated parallel DNN training (top: forward pass, middle/bottom: weight gradient computation) using a 2×3 process grid indexed as P_{ij} .

$$\begin{aligned}
T_{comm} = & 3 \sum_{i \in L_M} \left(\alpha \lceil \log(P_r) \rceil + |B| \frac{P_r - 1}{P_r} \beta \frac{d_i}{P_c} \right) + \\
& 2 \sum_{i \in L_M} \left(\alpha \lceil \log(P_c) \rceil + \frac{P_c - 1}{P_c} \beta \frac{|W_i|}{P_r} \right) + \\
& \sum_{i \in L_D} \left(\alpha + \beta \frac{|B|}{P_c} X_W^i X_C^i \lfloor k_h^i / 2 \rfloor \right) + \\
& \sum_{i \in L_D} \left(\alpha + \beta \frac{|B|}{P_c} X_W^{i+1} X_C^{i+1} \lfloor k_w^i / 2 \rfloor \right) + \\
& 2 \sum_{i \in L_D} \left(\alpha \lceil \log(P) \rceil + \frac{P - 1}{P} \beta |W_i| \right),
\end{aligned} \tag{6}$$

where L_M and L_D refer to the list of layers where the P_r groups are used to partition either the model or the domain. Note that for $L_M = L$, $L_D = 0$, we get the integrated model and batch parallel complexity as expected.

The choice of whether to partition the model or the domain can be made by computing the communication complexity. Generally, it is better to use domain parallelism for the initial layers of the network, since the activation size is large. However, the domain parallel approach loses its communication advantage for fully connected layers (for which $k_h = X_H$, $k_w = X_W$).

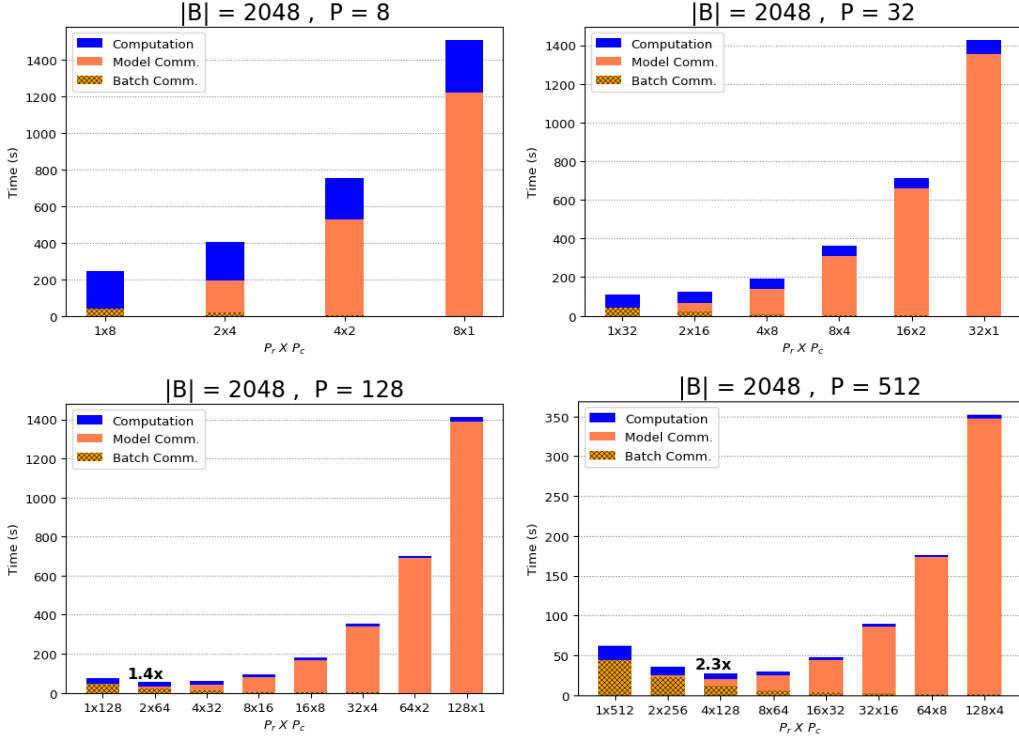


Figure 6: Strong scaling analysis of integrated model and batch parallel using the simulated results. The speedup compared to pure batch parallel is shown in bold text on top of the best bar chart. In strong scaling, we keep the global batch size fixed, and increase the number of processes to reduce the training time. For small number of processes, where per process batch size is close to optimal, the pure batch parallel provides the best running time complexity. However, as the number of processes increase, this per process batch size decreases to sub-optimal values. Here the integrated parallel approach automatically selects the best combination. For this reason, the speed up attained is higher for larger processor counts.

3 Simulated Performance in Training AlexNet

Simulation setup. We analytically explore the spectrum of both the integrated batch and model parallel approach as well as the full integration with domain parallelism by simulating Eq. 5 and Eq. 6. We show that the latter results in better performance for various scenarios as expected. To limit the number of variables, we fix a network (AlexNet), a training set of images (ImageNet LSVRC-2012 contest), and a computing platform (NERSC’s Cori supercomputer). These fixed options described in Table 1, are chosen just to develop a proof-of-concept of our integrated batch and model parallel approach. Next, we compute the communication time for a single iteration using Eq. 3 with various choices of the mini-batch size $|B|$, the number of processes, and the configuration of process grid $P_r \times P_c$. Finally, we compute the communication time for a complete epoch by multiplying the communication time from Eq. 3 by $N/|B|$.

Furthermore, we experimentally measured the computational time needed for an SGD iteration on single KNL using Intel Caffe. Based on the single-KNL measurement for different mini-batch sizes, we project the computational time on higher process counts and show them in the subsequent results.

Strong scaling with a fixed mini-batch size. At first, we present the strong scaling results for integrated model and batch parallel in Fig. 6 where the training was performed using $P = 8$ to $P = 512$ processes with a fixed mini-batch size of 2,048. In each subfigure in Fig. 6, only the configurations of the process grid vary.

Figure 6 shows that the better performance can be attained with an integrated batch and model parallelism, especially on higher concurrency. For example, on 512 processes, the best performance is

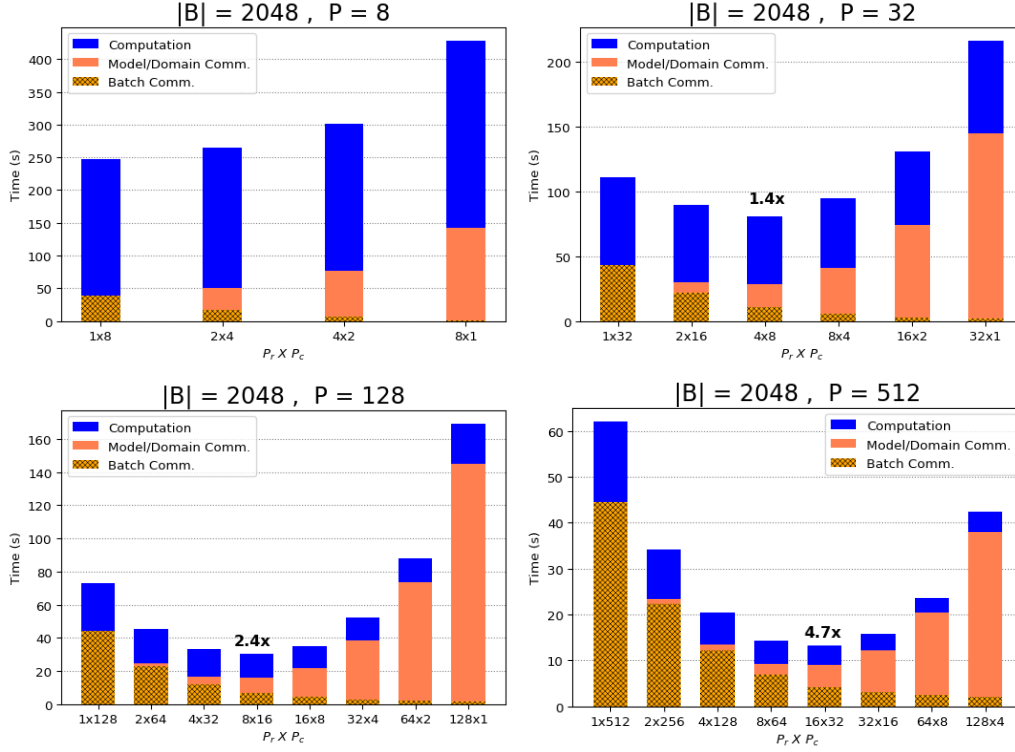


Figure 7: Strong scaling analysis of the full integrated model, batch, and domain parallel using the simulated results. The speedup compared to pure batch parallel is shown in bold text on top of the best bar chart. Notice the significant improvement in best time compared to Fig. 6 which only uses integrated model and data parallel.

	Fixed options	Relevant Parameters
Network architecture	AlexNet [13]	5 convolutional and 3 fully connected layers parameters: 61M
Training images	ImageNet LSVRC-2012 contest	Number of training images: 1.2M Number of categories: 1000
Computing platform	NERSC's Cori2	Processor: Intel Knights Landing (KNL) latency: $\alpha = 2\mu s$ inverse bandwidth: $1/\beta = 6GB/s$

Table 1: Fixed parameters used to simulate the cost of training neural networks using integrated batch and model parallel approach. We only change the mini-batch size and the number and configurations of processes in the presented results.

observed with 4×128 process grid, as shown in Figure 6(d). The improved performance is primarily driven by reduced communication needed by the integrated model and batch parallel approach (Eq. 5). However, the benefit of the integrated approach is not realized on a relatively low concurrency, such as with 8 processes in Figure 6(a). The reason behind this is that the $|W_i|/P_r$ term in the communication cost of model parallelism cannot be hidden with a small value of P_r .

The integrated approach helps reduce the computational time as well. As one can see, for pure batch parallel approach with $P = 8$ in Figure 6(a), every process gets a batch size of $2048/8 = 256$ for the local forward and backwards pass. A local batch size of 256 leads to the optimal performance on KNL as demonstrated in Fig. 4. As the number of processes increases, the per-process batch size decreases, leading to sub-optimal performance (see Fig. 4). The integrated approach can partially mitigate this by replicating a batch of training examples among P_r processes. Hence, the integrated

parallel approach can take advantage of the available hardware resources by automatically selecting the best configurations for distributing training examples, resulting in faster training of neural networks.

We also show how the results improve by using the full integrated approach where we integrate model, batch, and domain parallel methods as shown in Fig. 7. Here for each layer, we decide whether to use the P_r group of processes to either partition the model or the input domain. The latter is preferred for convolutional layers for which the activation size is large. For such cases, the communication overhead of the model parallel would make it sub-optimal. However, for fully connected or layers for which the activation size is small, it is beneficial to use model parallel approach. Overall, integrating all three forms of parallelism leads to the best results, as evident by comparing Fig. 7 and Fig. 6. The same trend holds for weak scaling analysis, as discussed below.

Scaling with a variable mini-batch size. We now consider scaling the mini-batch size and the process grid simultaneously and show the results in Fig. 8, and Fig. 9, respectively. In each corresponding subfigure, only the configurations of the process grid vary for a fixed P and $|B|$. Similar to Fig. 6 and Fig. 7, the integrated parallel approach can find a balanced mixture of model and batch parallelism that can substantially expedite the training of neural networks. Again the full integrated model, batch and domain parallel approach results in best performance as compared to only pure model or data parallel methods.

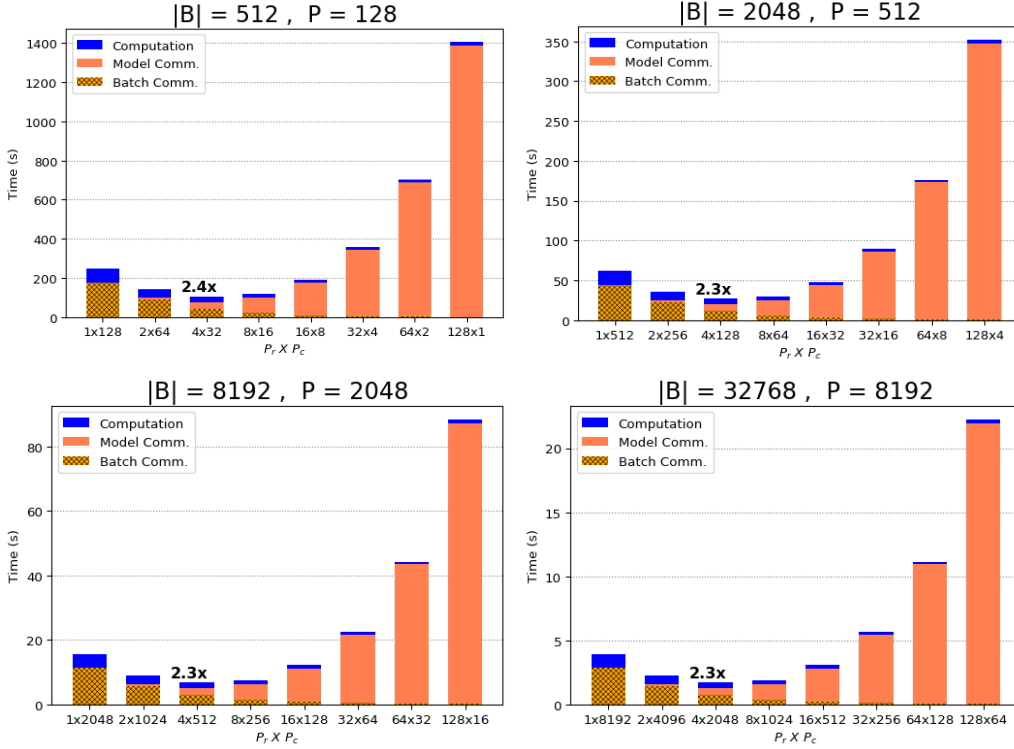


Figure 8: Simulated cost of integrated model and batch parallel method. We present weak scaling results for the communication and computation complexity when training AlexNet. The red bar shows the total communication time, with the cross hatched portion representing the time spent in batch parallel communication (i.e. the ring all-reduce during backprop). The speedup compared to pure batch parallel is shown in bold text on top of the best bar chart.

4 Discussion

Most DNN architectures have convolutional, fully connected, and sparse layers. Hence, the relative communication cost of model, batch, or domain parallel terms in the integrated model changes depending on the type of layer. For fully connected layers, $|W|_i = d_{i-1}d_i$, hence the ratio of

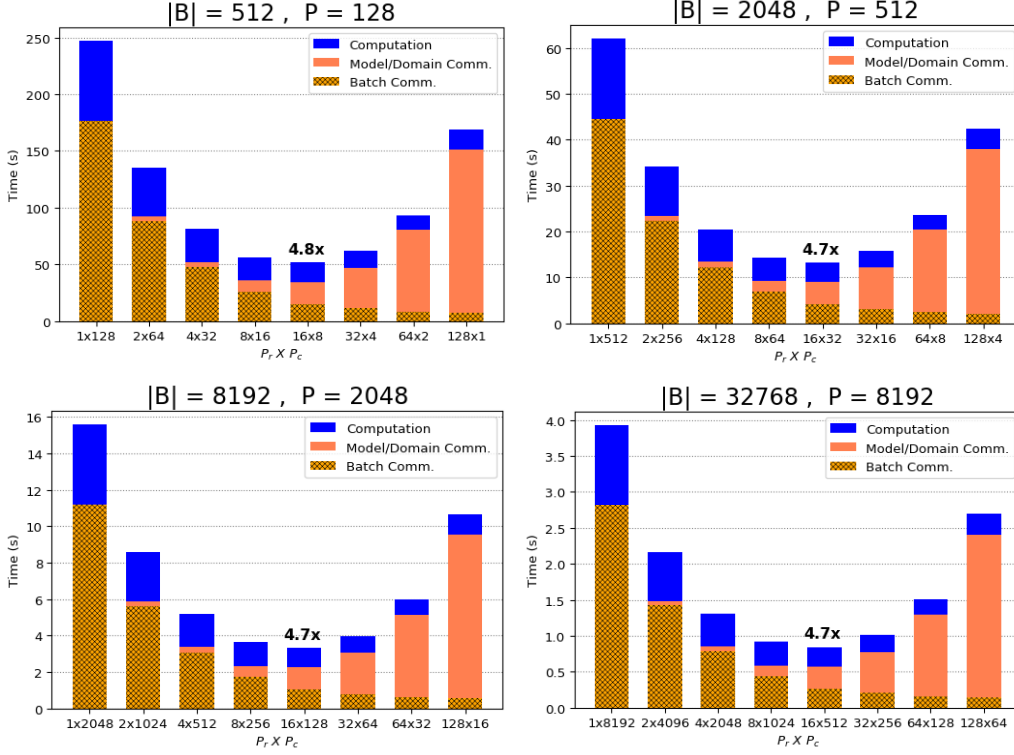


Figure 9: Weak scaling results for the full integrated model, batch, and domain parallel. The speedup compared to pure batch parallel is shown in bold text on top of the best bar chart. Notice the improved performance compared to Fig. 8, which only uses model and data parallelism.

communication in model parallelism to batch parallelism for a single layer is $|B|/d_{i-1}$. The situation with unstructured sparse layers is similar to the fully connected case, but this time the relative communication ratio between model and batch parallelism is scaled proportional to the sparsity percentage. For convolutional networks, $|W|_i = (k_h k_w c^{in}) c^{out}$ where the convolution kernel is of dimensions $k_h \times k_w$ and c^{in} (c^{out}) is the number of input (output) channels. The output channel size is the number of distinct kernels used in this layer. The input channel size is the number of distinct kernels used in the previous layer or (first layer) the number of channels in the input image. For the convolution layers, the domain parallel approach only needs to communicate a small ghost region, which has a much smaller communication volume as compared to the model parallel approach. This is especially the case for the initial layers of the network where the height and width of the activation is large and the number of channels is relatively small.

In the light of these observations, one can use different $P_r \times P_c$ grids for different layers of the network, but that requires a data redistribution in between. In our simulations, we use the same process grid for every layer for simplicity. We see that the integrated approach has lower communication cost for different batch values, and results in smallest training time per epoch even when we do not use different $P_r \times P_c$ for each layer.

5 Conclusion

We presented a 1.5D and a 2.5D integrated parallel algorithm that exploits model, batch, and domain parallelism. We discussed the associated communication complexity by analyzing both forward and backwards pass, and showed that theoretically the integrated parallel approach can achieve better run time. Furthermore, the integrated parallel approach increases the scalability limit of the pure batch parallel method that is commonly used, by decomposing both along the weight matrix as well as the domain. This approach allows optimal selection of per process batch size and model size which results in better throughput as compared to pure batch/model parallel algorithms.

References

- [1] Grey Ballard, James Demmel, Olga Holtz, and Oded Schwartz. Minimizing communication in numerical linear algebra. *SIAM Journal on Matrix Analysis and Applications*, 32(3):866–901, 2011.
- [2] Lynn Elliot Cannon. *A cellular computer to implement the Kalman filter algorithm*. PhD thesis, Montana State University, 1969.
- [3] Ernie Chan, Marcel Heimlich, Avi Purkayastha, and Robert Van De Geijn. Collective communication: theory, practice, and experience. *Concurrency and Computation: Practice and Experience*, 19(13):1749–1783, 2007.
- [4] Trishul M Chilimbi, Yutaka Suzue, Johnson Apacible, and Karthik Kalyanaraman. Project adam: Building an efficient and scalable deep learning training system. In *OSDI*, volume 14, pages 571–582, 2014.
- [5] Adam Coates, Brody Huval, Tao Wang, David Wu, Bryan Catanzaro, and Ng Andrew. Deep learning with COTS HPC systems. In *International Conference on Machine Learning*, pages 1337–1345, 2013.
- [6] Dipankar Das, Sasikanth Avancha, Dheevatsa Mudigere, Karthikeyan Vaidynathan, Srinivas Sridharan, Dhiraj Kalamkar, Bharat Kaul, and Pradeep Dubey. Distributed deep learning using synchronous stochastic gradient descent. *arXiv preprint arXiv:1602.06709*, 2016.
- [7] Jeffrey Dean, Greg Corrado, Rajat Monga, Kai Chen, Matthieu Devin, Mark Mao, Andrew Senior, Paul Tucker, Ke Yang, Quoc V Le, et al. Large scale distributed deep networks. In *Advances in neural information processing systems*, pages 1223–1231, 2012.
- [8] Priya Goyal, Piotr Dollár, Ross Girshick, Pieter Noordhuis, Lukasz Wesolowski, Aapo Kyrola, Andrew Tulloch, Yangqing Jia, and Kaiming He. Accurate, large minibatch SGD: Training ImageNet in 1 hour. *arXiv preprint arXiv:1706.02677*, 2017.
- [9] Mohammad Havaei, Axel Davy, David Warde-Farley, Antoine Biard, Aaron Courville, Yoshua Bengio, Chris Pal, Pierre-Marc Jodoin, and Hugo Larochelle. Brain tumor segmentation with deep neural networks. *Medical image analysis*, 35:18–31, 2017.
- [10] Kaiming He, Xiangyu Zhang, Shaoqing Ren, and Jian Sun. Deep residual learning for image recognition. In *Proceedings of the IEEE conference on computer vision and pattern recognition*, pages 770–778, 2016.
- [11] Peter H Jin, Qiaochu Yuan, Forrest Iandola, and Kurt Keutzer. How to scale distributed deep learning? *arXiv preprint arXiv:1611.04581*, 2016.
- [12] Penporn Koanantakool, Ariful Azad, Aydın Buluç, Dmitriy Morozov, Sang-Yun Oh, Leonid Oliker, and Katherine Yelick. Communication-avoiding parallel sparse-dense matrix-matrix multiplication. In *Proceedings of the IPDPS*, 2016.
- [13] Alex Krizhevsky, Ilya Sutskever, and Geoffrey E Hinton. Imagenet classification with deep convolutional neural networks. In *Advances in neural information processing systems*, pages 1097–1105, 2012.
- [14] Jonathan Long, Evan Shelhamer, and Trevor Darrell. Fully convolutional networks for semantic segmentation. In *Proceedings of the IEEE Conference on Computer Vision and Pattern Recognition*, pages 3431–3440, 2015.
- [15] A. Mang, S. Tharakan A. Gholami, N. Himthani, S. Subramanian, J. Levitt, M. Azmat, K. Scheufele, M. Mehl, C. Davatzikos, B. Barth, and G. Biros. SIBIA-GIS: Scalable biophysics-based image analysis for glioma segmentation. *The multimodal brain tumor image segmentation benchmark (BRATS), MICCAI*, 2017.
- [16] Benjamin Recht, Christopher Re, Stephen Wright, and Feng Niu. Hogwild: A lock-free approach to parallelizing stochastic gradient descent. In *Advances in neural information processing systems*, pages 693–701, 2011.

- [17] Shaoqing Ren, Kaiming He, Ross Girshick, and Jian Sun. Faster R-CNN: Towards real-time object detection with region proposal networks. In *Advances in neural information processing systems*, pages 91–99, 2015.
- [18] RO Rogers and David B Skillicorn. Using the BSP cost model to optimise parallel neural network training. *Future Generation Computer Systems*, 14(5):409–424, 1998.
- [19] Christian Szegedy, Wei Liu, Yangqing Jia, Pierre Sermanet, Scott Reed, Dragomir Anguelov, Dumitru Erhan, Vincent Vanhoucke, and Andrew Rabinovich. Going deeper with convolutions. In *Proceedings of the IEEE conference on computer vision and pattern recognition*, pages 1–9, 2015.
- [20] Rajeev Thakur, Rolf Rabenseifner, and William Gropp. Optimization of collective communication operations in MPICH. *The International Journal of High Performance Computing Applications*, 19(1):49–66, 2005.
- [21] Robert A Van De Geijn and Jerrell Watts. SUMMA: Scalable universal matrix multiplication algorithm. *Concurrency-Practice and Experience*, 9(4):255–274, 1997.
- [22] Bichen Wu, Forrest Iandola, Peter H Jin, and Kurt Keutzer. Squeezedet: Unified, small, low power fully convolutional neural networks for real-time object detection for autonomous driving. *arXiv preprint arXiv:1612.01051*, 2016.
- [23] Bichen Wu, Alvin Wan, Xiangyu Yue, and Kurt Keutzer. Squeezeseg: Convolutional neural nets with recurrent crf for real-time road-object segmentation from 3d lidar point cloud. In *In Review*, 2017.
- [24] Yang You, Zhao Zhang, C Hsieh, James Demmel, and Kurt Keutzer. ImageNet training in minutes. *CoRR*, abs/1709.05011, 2017.
- [25] Sixin Zhang, Anna E Choromanska, and Yann LeCun. Deep learning with elastic averaging SGD. In *Advances in Neural Information Processing Systems*, pages 685–693, 2015.

6 Appendix: Detailed Derivations

6.1 Detailed Derivation of the Forward Pass

During the forward pass for data parallel, each process reads a mini-batch size of $|B|/P$ input images and the calculations are performed as follows:

$$Y_i = W X_i, \quad (7)$$

where X_i and Y_i is the i th column of X and Y , respectively. Here, W is shared and no communication is needed. However, in the model parallel case we have:

$$Y_{p,i} = W_p X_i, \quad (8)$$

where p denotes the process id, W_p is the fraction of weights in each process, and $Y_{p,i}$ is the fraction of output activation computed locally. This local component needs to be communicated via an all-gather operation to concatenate all partial activations for the next layer’s computation.

6.2 Detailed Derivation of Backpropagation

During backpropagation, the gradient of the loss functional with respect to output activations Y is given ($\Delta_Y = \frac{d\mathcal{J}}{dY}$), and one has to compute the gradient with respect to the weights (Δ_W) as well as the input feature map (Δ_X). The latter is needed for propagating the gradient to lower layers. We use capital letters for input and output activation as we are mostly interested in the mini-batch setting $B > 1$. Using chain rule we have:

$$\Delta_W = \frac{d\mathcal{J}}{dW} = \sum_{i=1}^{|B|} \frac{d\mathcal{J}}{dY_i} \frac{dY_i}{dW} = \sum_{i=1}^{|B|} \frac{d\mathcal{J}}{dY_i} X_i^T = \Delta_Y X^T, \quad (9)$$

Now in the distributed case, we have:

$$\frac{d\mathcal{J}^p}{dW} = \sum_{i=1}^{|B|/P_c} \frac{d\mathcal{J}}{dY_i} X_i^T, \quad (10)$$

$$\frac{d\mathcal{J}}{dW} = \sum_{k=1}^{P_c} \frac{d\mathcal{J}^p}{dW}. \quad (11)$$

where p is the process id. Notice that the last step requires an all-reduce between P_c processes, but no communication is needed for the model parallel part as the input activation is already communicated via the all-gather collective of forward pass. To backpropagate the gradient, one needs to compute $\Delta_X = \frac{d\mathcal{J}}{dX}$ as well. We derive it for one column of Δ_X below as each column can be computed independently:

$$\Delta_{X_i} = \frac{d\mathcal{J}}{dX_i} = \frac{d\mathcal{J}}{dY_i} \frac{dY_i}{dX_i} = W^T \frac{d\mathcal{J}}{dY_i} = W^T \Delta_{Y_i}, \quad (12)$$

Here in the distributed model parallel part, the weight matrix is distributed among P_r processes. To backpropagate the gradient, every process computes its contribution to the gradient followed by an all-reduce collective between P_r processes:

$$\frac{d\mathcal{J}^p}{dX_i} = W^T \frac{d\mathcal{J}}{dY_i}, \quad (13)$$

$$\frac{d\mathcal{J}}{dX_i} = \sum_{k=1}^{P_r} \frac{d\mathcal{J}^k}{dX_i}. \quad (14)$$